since 1961

Baltica

BALTICA Volume 36 Number 1 June 2023: 37–50
https://doi.org/10.5200/baltica.2023.1.4

3D data integration for geo-located cave mapping based on unmanned aerial vehicle and terrestrial laser scanner data

Resul Çömert*, Samed Özdemir, Burhan Baha Bilgilioglu, Selçuk Alemdag, Halil Ibrahim Zeybek

Çömert, R., Özdemir, S., Bilgilioglu, B.B., Alemdag, S., Zeybek, H.I. 2023. 3D data integration for geo-located cave mapping based on unmanned aerial vehicle and terrestrial laser scanner data. *Baltica*, *36 (1)*, 37–50. Vilnius. ISSN 1648-858X.
Manuscript submitted 13 December 2022 / Accepted 12 April 2023 / Available online 19 May 2023

Abstract. The Akçakale cave is a significant natural and cultural heritage site in the Black Sea region of eastern Turkey. The complex geometry and difficult-to-access areas of the cave have made the use of traditional mapping methods challenging. To overcome these limitations, this study utilized TLS and UAV technology to produce highly accurate 2D and 3D data for cave management and risk assessment purposes. The TLS system was used to create a detailed 3D point cloud of the cave interior, while the UAV system generated a 3D model of the surface topography outside the cave. The two sets of data were combined in the GIS environment using a geodetic network established in the study area, providing a common geodetic reference system for both TLS and UAV data. The study found that the cave area is 13,750 m^2, which is smaller than the area of 18,000 m^2 that was previously estimated using conventional measurement methods. The volume and ceiling heights of the cave were calculated using the elevation models generated from TLS point cloud data. The 3D point cloud data were also used to map dripstone locations on the floor and ceiling of the cave, and the boundaries of rock blocks on the ground were precisely determined. The study identified potential risks associated with the cave, particularly the risk of rockfall in the source rock areas around the cave entrance and the southern part of the cave. The nearest building to the cave is approximately 35 meters away, and all the buildings in the area are less than 300 meters from the cave. In the event of the cave collapse, the buildings in the southern part of the cave are at risk of rockfall. This study demonstrates the effectiveness of combining data from TLS and UAV systems to generate broad and sensitive cave mapping and risk assessment data, which are critical for cave management and safety. The collected data can be used for cave stability investigations and rockfall risk assessments. This study provides a foundation for future explorations of the Akcakale cave and highlights the potential for modern surveying techniques to enhance our understanding of complex geological structures such as caves.

Keywords: *cave formations; TLS; UAV; rock fall; point cloud*

*Resul Çömert** *(rcomert@eskisehir.edu.tr)* *https:// orcid.org/ 0000-0003-0125-4646*
Eskisehir Technical University, Institute of Earth and Space Sciences, Eskisehir, 26555, Turkey;

Samed Özdemir *https:// orcid.org/ 0000-0001-7217-899X*
Gümüşhane University, Department of Geomatic Engineering, Gümüşhane 29100, Turkey;

Burhan Baha Bilgilioglu *https:// orcid.org/ 0000-0001-6950-4336*
Gümüşhane University, Department of Architecture and Urban Planning, Gümüşhane 29100, Turkey;

Selçuk Alemdag *https:// orcid.org/ 0000-0003-2893-3681*
Gümüşhane University, Department of Geological Engineering, Gümüşhane 29100, Turkey;

Halil Ibrahim Zeybek *https:// orcid.org/ 0000-0002-4097-9079*
Ondokuz Mayıs University, Department of Geography, Samsun 55105, Turkey

**Corresponding author*

INTRODUCTION

Cave surveying is an essential process for numerous purposes such as cave mapping, 3D modeling, examination of cave morphology, and investigation of cave stability (Albert 2017). Since caves are subsurface formations, it is very difficult to measure caves in detail using classical methods, due to the irregular geometric shapes, high ceilings, and insufficient lighting conditions in caves (Lindgren, Galeazzi 2013). Cave mappings are carried out applying traditional measurement methods, caves are usually represented as longitudinal or cross sections, and the details on the floor of the caves are presented on a 2D map (De Waele *et al*. 2018). Nowadays, with the low cost of access and the ability to capture a large 3D scene quickly and accurately in a session, high-resolution 3D measurement systems such as TLS are being widely adopted for detail-rich cave representation instead of traditional methods. The ability of advanced measurement systems to represent the cave morphology in unprecedented detail made them indispensable tools for the morphological examination of caves, determination of their stability against collapse, and detailed 3D representation of caves (Lindgren, Galeazzi 2013; Armstrong *et al.* 2018).

Terrestrial laser scanner (TLS) systems have been used effectively in cave measurements in recent years. TLS has become an effective system for producing 3D information about the floor, walls, and ceilings of caves with the ability to collect data in a lightless, complex environment and to produce thousands of 3D points per second (Idrees, Pradhan 2016). There are applications such as 3D modeling and mapping of caves (Gallay *et al*. 2015; Fabbri *et al*. 2017), morphological analysis (Fabbri *et al*. 2017; De Waele *et al*. 2018), cave stability analysis (Idrees, Pradhan 2018) and understanding of cave systems (upinský *et al*. 2022; Hoffmeister *et al*. 2016) using the TLS measurements. In addition, there are studies in which TLS and terrestrial photogrammetry methods are used together to produce cave models (Pukanská *et al*. 2020; De Waele *et al*. 2018). In these studies, TLS systems have been shown to provide effective results in extracting detailed 3D information about caves.

Cave systems are complex geological formations that are subject to various risks such as collapses and rockfalls due to cave instability. Therefore, in order to assess potential risks and take necessary precautions, it is crucial to determine the relationship of the cave with the surface topography. In the last decade, unmanned aerial vehicles (UAVs) emerged as an essential tool for 3D mapping due to their ability to generate high-resolution 2D and 3D maps, including orthophotos, Digital Elevation Models (DEM), and point clouds, using a wide range of imaging and depth sensors. This technology enables easy and cost-effective deployment over any type of terrain, including areas where human access would be dangerous. UAV systems have been used in various applications including investigations into the effects of loess cave development on landslides and geomorphological processes (Hu *et al*. 2020), 3D data generation for internal and external cave modelling (Alessandri *et al*. 2020), determination of the cave openings developed in volcanic regions (Sam *et al*. 2020). While TLS systems provide highly detailed 3D data for cave interiors, UAVs can generate accurate topographic maps outside the cave, which can be utilized for analyzing the interaction between the cave and the surface topography. These studies have shown that UAV systems can successfully generate accurate data for the surface topography of the cave. The integration of the data obtained from these two systems provides critical information when conducting 3D analyzes in studies where the interior morphology of the cave and the surface topography should be evaluated together. A review of past cave papers using integrated UAV and TLS systems to generate data from inside and outside the cave shows that there is only one study in the literature that has analyzed the stability of man-made monastery caves (Domej *et al*. 2022). The present study is the first one to analyze the internal and external relationship of a natural cave with complex geometry using TLS and UAV systems.

This study aims to precisely map the internal morphological formations and surface topography of the Akçakale natural formation cave located in the Gümüşhane province of Turkey, which is planned to be opened as a showcase for tourists in the future, to obtain reference data for subsequent deformation studies using TLS and UAV systems. This study contributes to the field of cave mapping and risk assessment by demonstrating the efficacy of modern surveying techniques, such as TLS and UAV technology, in generating highly accurate and detailed data for cave management and risk assessment. This study provides a comprehensive understanding of the Akcakale cave's geometry and characteristics, such as its area, volume, and potential areas of instability. The study also underlines the importance of collecting data from multiple sources and their integration into a GIS environment for producing a complete and accurate map of the cave and its surroundings. The findings of this study can serve as a guide for future research and help enhance cave management and safety practices.

STUDY AREA

The Akçakale cave is located within the borders of the Arsa neighborhood of the Akçakale village, which is approximately 10 km away from the Gümüşhane

city center in Turkey (Fig. 1). The cave was discovered in 1996 and its first mapping was carried out using classical surveying methods (Uzun, Zeybek 1996). The cave was documented as a natural asset-group B cave by the Ministry of Environment and Urbanization of the Republic of Turkey in 2021. B-group caves are defined as the ones that are important in terms of natural aesthetics, science and ecology, and can be used for health and eco-tourism purposes, considering the natural balances and disaster risks.

The climatological features of the cave exterior are semi-arid climatic conditions. The annual average temperature is 9.7 °C and the daily temperature amplitude exceeds 20 °C. The annual average precipitation in the region is 460 mm. Precipitation comes in the form of snow in winter. The temperature inside the cave is cooler than outside in summer, and warmer in winter. The temperature values measured inside the cave in summer are between 14°C and 18°C. The humidity measured in summer months varies between 54% and 74% (Uzun, Zeybek 1996).

The Akçakale cave is situated within the Berdiga Formation as a geological unit that has off-white-, grey-, and beige-colored, medium-thick, and massive lithological layers. At the top, this Berdiga Formation comprises clayey limestones with light-grey fresh surfaces, brownish weathering surfaces, and karst dissolution cavities, while at the bottom, dolomitic limestones can be found. Dolomites and dolomitic limestones are found at the base of the Berdiga Formation

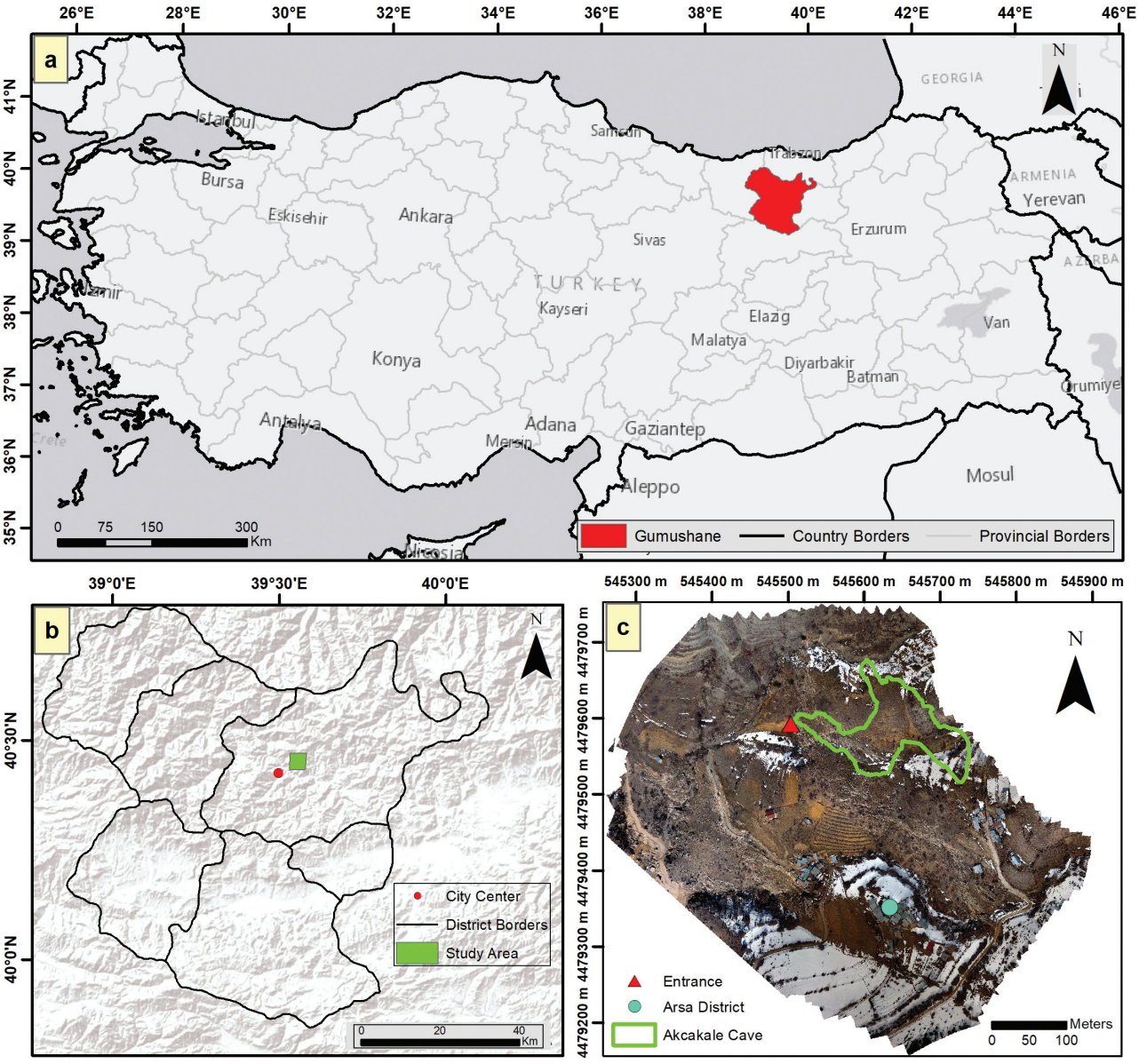

Fig. 1 Location map of the study area: (a) the Gümüşhane province in Turkey (Backround map sources: ESRI basemaps from ArcGIS online); (b) location of the study area in the Gümüşhane province (Backround map sources: ESRI basemaps from ArcGIS online); (c) location of the Akçakale cave, cave entrance and the Arsa District on the orthophoto map produced by UAV

and further up with limestones. Being enriched with magnesium, the lower limestones are dolomitized and hardened. In places, dolomites, which are of thin-bedded and sandy texture, are covered by thick-bedded limestones. Limestone fractures are filled with local calcite. The weathering surfaces with dissolution cavities are in reddish-brown shades. The study area, where in some places the inclination angle of the slopes exceeds 65°, is frequently and deeply broken by the Doğankent Stream branches. Formation of abundant dripstones (stalactites, cave pearls, cave flowers, cave wall travertines, and flowstone) is taking place in the Akçakale Cave, which is due to the ongoing karst limestone dissolution induced by ambient conditions. The main gallery of the cave extends in the northeast direction followed by secondary galleries extending in the northwest and southeast directions (Alemdag *et al*. 2019). The images of the cave measurement process are presented in Fig. 2.

MATERIALS AND METHODS

Figure 3 illustrates the methodology followed in this study, and Figure 4 shows the instruments used for performing measurements. During the field measurements, the researchers used a terrestrial laser scanning system to measure the cave interior and an unmanned aerial vehicle (UAV) system to take aerial

Fig. 2 Images of the entrance to the cave and its interior

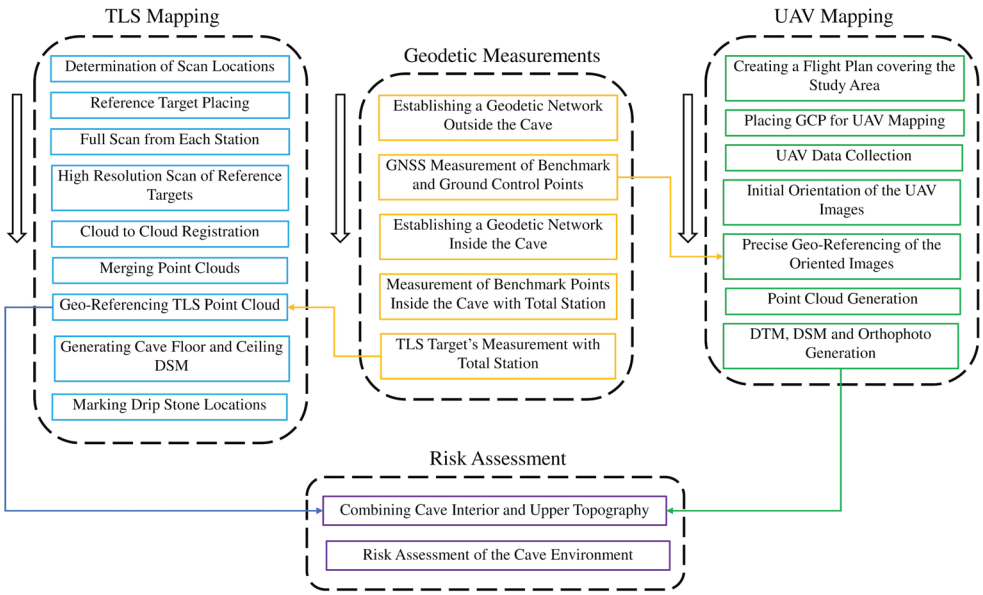

Fig. 3 Workflow of the study

photos and to evaluate the surface topography of the cave (Fig. 4). The processing of the data obtained from the TLS and UAV systems, the mapping of the cave interior and the surface topography as well as the analysis of the relationship between the cave interior and the surface topography were performed in the office.

To merge the 3D measurements taken both inside and outside the cave into a common reference system, a ground-based geodetic network was established that covered the area surrounding the cave exterior and extended to the end of the cave. The establishment of the network started with the installation of two reference points, named P1 and P2, which were placed near the cave entrance, fixed to the ground and measured using the GNSS-RTK method. Then, a geodetic network from the point P2 to the end of the cave, with P1 as a reference point, was established using a laser total station that was installed at the point P2. As the cave entrance was narrow and steep, finding a suitable location for the third reference point, P3, was challenging. The researchers placed the total station as low as possible at the point P3 and used precise reflectors to locate the cave floor and to identify a suitable location for the fourth reference point, P4. The total station was then placed at the point P4 inside the cave and P3 as a reference point. A total of seven points were established, including the point P4. The TLS targets, which were attached to the cave walls, were used to align the TLS point clouds to the geodetic reference system that was measured using the total station at each point. Outside the cave, ground control points (GCPs) were installed on the ground (Fig. 4) and measured using the GNSS-RTK method to convert UAV data into a common reference system.

The Interior of the cave was measured using the Leica ScanStation C10 TLS system, which is capable of measuring up to 50000 points per second and operates on the principle of time of flight (ToF) measurement. The scanner has 360° horizontal and 270° vertical viewing angles, and the measurement accuracy ranges from 4–6 mm to 50 m. A high-resolution digital camera on the scanner is used to colourize the scanner-collected 3D points (Leica Geosystems AG 2011). In this study, it was impossible to use an integrated digital camera of the TLS due to the pitch-black condition inside the cave. Due to rockfalls, the cave floor was covered with large rock blocks, making movement difficult. In addition, it was hard to establish suitable station positions for the laser scanner on such a rough surface. Before conducting the laser scanning in the cave, we were concerned about the high humidity inside the cave compared to that outside, as it might negatively impact the accuracy and operational performance of the terrestrial laser scanner. However, having conducted the scan and assessed the data, we discovered that despite the challenging conditions, the scanner performed admirably. This fact indicates that the high humidity inside the cave had no substantial impact on the accuracy or operational performance of the scanner. During the laser scanning process, we noticed that at some points water was leaking from the cave ceiling. While these leaks were visible in the point cloud data derived from a few of the stations, we did not observe any negative effects on the quality of the overall scan results. In other words, the leaks did not seem to have a significant impact on the accuracy or usability of the scans. The team used target markers affixed to the cave walls for both combining the TLS point clouds and geo-referencing the combined point clouds with subsequent geodetic measurements. Specifically, the Leica standard targets printed on paper were attached to the cave walls to align the laser scans. We were concerned about the accuracy of the alignment because of the high humidity within the cave, due to

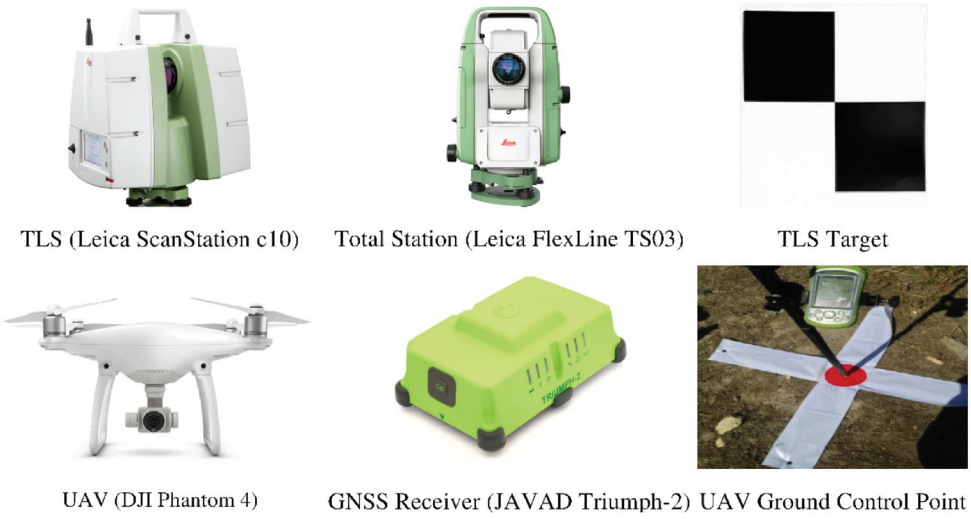

Fig. 4 Instruments used in the field survey for the cave mapping campaign

which the targets could have soon become wet, their utility being reduced. Upon examination of the data, it was determined that the high humidity had no real impact on the target measurements. The geodetic coordinates of the targets affixed to the cave walls were determined using the Leica FlexLine TS03 total station equipped with the non-prism laser measurement mode. The TLS data processing was conducted using the Leica Cyclone 9.2 Education version software. During the processing phase, multiple TLS point clouds of the cave interior were registered and integrated using the cloud-to-cloud registration method available in the Leica Cyclone software. Moreover, the combined point cloud was geo-referenced using the target marker coordinates obtained from the terrestrial measurements performed using the total station.

The Phantom 4 UAV system, which consists of a 12 MP digital camera, a Global Positioning System (GPS), and an onboard Inertial Measurement Unit (IMU) system, was used to map the surface topography of the cave. The process of UAV photogrammetric data production involves the following stages: flight planning, establishment and measurement of ground control points (GCPs), image acquisition, and image processing. The accuracy of the photogrammetric products highly depends on the overlap between the adjacent images and stability of the flight path, which requires the autopilot software to precisely control the UAV on a determined flight path. To this end, a flight plan was created by specifying the flight altitude, the ground sampling distance, forward and side overlaps in the Pix4D Capture software to ensure a steady flight path and a consistent overlap between the images. Also, Pix4D Capture is used as the autopilot software for the UAV. During the flight, the camera center coordinates and the exterior orientation information of every image taken along the flight path were recorded using the GPS and IMU instruments. The root-mean-square error (RMSE) of the products produced by the processing of aerial photos obtained from DJI Phantom with GCPs is below 5 cm horizontally and between 5–6 cm vertically. (Öztürk *et al*. 2017; Chaudhry *et al*. 2020; Le *et al*. 2020).

Since the positioning accuracy of the UAV onboard GPS is low, the homogeneously distributed GCPs are placed in the flight area to produce high-accuracy data in the defined geodetic coordinate system. The coordinates of these GCPs are measured with a GNSS receiver. In this study, the Javad Triumph-2 GNSS receiver was used to measure the ground control points in the study area. GCPs coordinates were measured based on the Turkish National RTK-CORS system. In the UAV image processing stage, the captured images are oriented and georeferenced using GCP coordinates and the exterior orientation information acquired from the onboard INS instrument. After the orientation and initial processing had been accomplished, the dense point cloud, mesh model, digital elevation models, and the orthomosaic data of the study area were generated. In this study, the UAV image processing was carried out with the Agisoft Metashape v.1.5.1 software. The plan of the cave was drawn on the TLS point cloud using the AutoCAD 2023 software. The Autodesk ReCAP v.0.7 software was used to combine the 3D point clouds produced with TLS and UAV. The Cloud Compare was used for the extraction of such cave interior details as stalactites, stalagmites, and travertine, and for the DEM generation of the cave floor, wall, and ceiling. The cave data generated using different software were transferred to the ArcGIS 10.8 GIS software, and the map of the cave interior and surface topography, the height differences between the cave floor, ceiling, and surface topography, volume calculations were carried out in the GIS environment.

The Akçakale cave formed within the limestones. Highly inclined limestone blocks are exposed in the surface topography of the cave, i.e., at the entrance of the cave and in the close vicinity of the cave boundary.

In order to determine the source rock area where rockfalls may occur, a detailed field study, satellite, orthophoto, and aerial photographs should be used. For the determination of the source rock areas, previous rockfall events and their traces on the slope/slope surface can be used. In addition, stress cracks in the upper elevations of slopes and slopes, discontinuity surfaces, and block accumulations due to falling at the lower parts of the slopes can be exploited. In this study, source rock areas were calculated according to equation 1 using the DTM (Žabota *et al*. 2019) generated from the UAV point cloud (Bauerhansl *et al*. 2010). Thus, the source rock area depending on a numerical parameter was determined together with the field observations for the study area.

$$ST = 55 * RES(DTM) - 0.075 \quad (1)$$

Where, ST indicates the slope threshold (ST) for the rockfall, and RES indicates the spatial resolution of the DTM in meters.

RESULTS

To map the Akcakale cave and determine its relationship with the surface topography, the interior of the cave was measured using the TLS system and the surface topography of the cave using the UAV system. The interior of the Akçakale Cave was scanned from six different positions, which were selected from safe and easy-to-reach locations providing a sufficient field of view for the TLS since most of the

interior of the cave is blocked by rocks falling from the ceilings and walls. Fourteen targets were placed on the walls of the cave to transform the point clouds from the scanner coordinate system to the geodetic coordinate system (Fig. 5). Starting from points P1 and P2 near the cave entrance, a geodetic network was established inside the cave by using the total station instrument to geo-reference the TLS point cloud. The coordinates of points P1 and P2 were measured using the GNSS-RTK method. After establishing the geodetic network, the target points affixed to cave walls were measured from each station with the total station using the non-prism laser measurement mode. Point clouds from six scan positions were registered with each other using the target points by applying the cloud-to-cloud registration method and merged into a single point cloud representing the interior of the cave in a local coordinate system. After the point clouds had been accurately registered and merged, the geo-referenced target coordinates were used to translate the local coordinate system of the point cloud into a geodetic coordinate system. The resulting point cloud data had 84 million points. The accuracy of 13 out of 14 targets was high enough to be used in the transformation process. In Table 1, the Root Mean Square Error (RMSE) of the target points was calculated at 15.4 cm on the X-axis, 16.3 cm on the Y-axis, and 10.6 cm on the Z-axis, while positioning errors of individual target points reached 21.4 cm, 20.6 cm, and 13.6 cm on the X, Y, Z axes, respectively. The positioning errors of the target points were higher than expected. The higher error rates were caused by the conditions inside the cave, i.e., insufficient lighting (during the geodetic measurements the targets were illuminated with a flashlight) and the rugged cave floor, which made it difficult to take measurements more precisely. However, this amount of error will have a minimal impact on the accuracy of the study since the main objective of the study was to successfully determine the immediate risk areas by associating the cave with the surface topography.

During the UAV data collection stage, 10 GCPs were placed in the study area before the flight and their coordinates were measured with a GNSS receiver using the GNSS-RTK method in the Turkish National CORS reference frame. To fully cover the whole study area, 4 flights were conducted, and 953 images were obtained. The photogrammetric products generated using the UAV imagery were georeferenced according to the GCPs coordinates, which were in the same geodetic coordinate system as the target points inside the cave. RMSE of the GCPs was 3.4 cm on the X axis, 3.7 cm on the Y axis, and

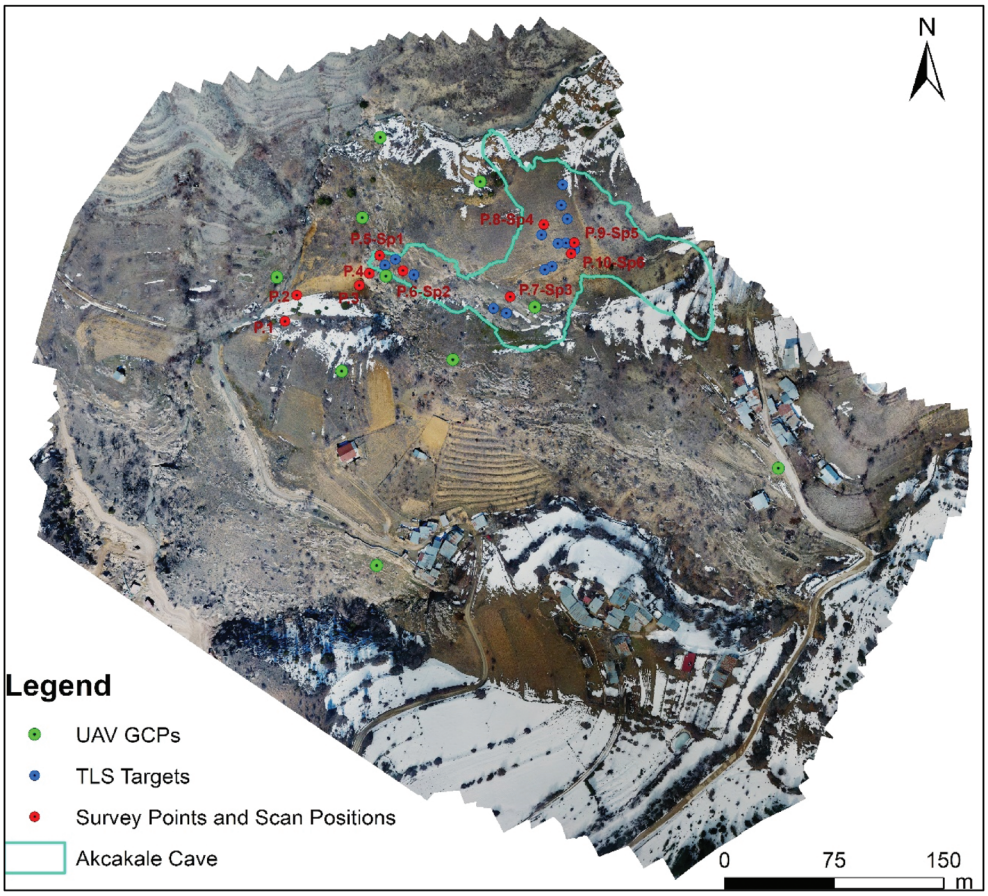

Fig. 5 Distribution of points used in TLS and UAV measurements of the Akçakale cave

4.3 cm on the Z axis, i.e., within the expected limits. During the data processing stage, a point cloud of approximately 18 million points, a 10 cm spatial resolution Digital Surface Model (DSM), and a 5 cm spatial resolution orthomosaic were created. After filtering out the non-ground points from the point cloud, a 10 cm spatial resolution DTM was created. The 3D TLS point cloud, the TLS point cloud and the UAV point cloud integration of the cave and the representation of the cave boundaries on the 3D hillshade are shown in Fig. 6.

For the cave interior mapping, the TLS point cloud was manually divided into two different point clouds. One of the point clouds represents the cave floor while the other point cloud the walls and the ceiling of the cave. The point cloud representing the cave floor was utilized to draw the 2D plan of the cave, to generate the DSM of the cave floor, and to extract locations of the dripstones (stalagmites and cave columns, dome-shaped stalagmites). The 2D plan of the cave was drawn using the AutoCAD 2023 software. The CloudCompare software was used for extracting dripstone locations and generating a 10 cm spatial resolution DSM of the cave floor. The point cloud data representing the walls and the ceiling of the cave were utilized to generate the DSM and to extract locations of stalactites on the cave ceiling. The final map of the cave was created in GIS environment by transferring the data produced using different software to the ArcMap 10.8 software.

The plan of the cave floor produced using the TLS point cloud data covers an area of 13 750 m^2 (Fig. 7a). The cave floor area stretching for approximately 150 m from the entrance is covered with rock blocks falling from the ceiling and walls (Figs 7a, 7c). Further away from that place in the cave, there appear such developed cave formations as stalagmites, cave columns and dome-shaped stalagmites. The absence of such formations as stalactites, stalagmites and cave columns, and dome-shaped stalagmites in this area is explained by falling rock blocks. These formations are densely located at the intersection between the main, northwest, and southeast galleries. There is a small lake in the gallery in the southeastern part of the cave. The place where this lake meets the wall is called the coast. Since the LiDAR beam does not reflect from the water surface, the lake area was approximately drawn over the point cloud. A few small-sized (20~30 cm) stalactites were found at the entrance of the cave. In the middle of the cave (Fig. 7b), it is possible to see 4~6 m-sized stalactites on the ceiling. In the areas where cave formations are dense, the size of stalagmites and cave columns varies from 1 to 5 m (Fig. 7d).

The study used DSM data obtained from the TLS to determine the height of the cave ceiling from the cave floor and to calculate the cave volume. The height of the cave ceiling was calculated by subtracting the upper DSM (cave walls and ceiling) from the cave floor DSM (Fig. 8a). The height of the cave ceiling was found to be lower at the cave entrance and in the main gallery, while the highest point of the cave ceiling (46.31 m) was recorded at the location leading to secondary galleries. The volume of the cave was calculated from DSMs and was found to be equal to 233,248.60 m^3. The surface topography DTM was created from the UAV imagery and the upper surface of the cave DSM was used for the calculation of the depth between the cave ceiling and the surface topography (Fig. 8b). The depth between the cave ceiling

Table 1 The error distribution of points used to locate TLS and UAV data in the Turkish National CORS geodetic coordinate system

TLS Targets Error				UAV GCPs Error			
	ΔX (m)	ΔY (m)	ΔZ (m)		ΔX (m)	ΔY (m)	ΔZ (m)
T_1	-0.093	0.128	0.017	GCP_1	-0.033	0.046	-0.021
T_2	-0.168	0.181	0.071	GCP_2	-0.037	-0.028	0.052
T_3	-0.137	0.091	0.012	GCP_3	0.048	0.035	-0.049
T_4	-0.102	0.179	0.071	GCP_4	0.055	-0.041	0.063
T_5	0.123	-0.102	-0.102	GCP_5	0.023	0.039	-0.036
T_6	-0.083	-0.115	0.140	GCP_6	-0.013	-0.027	0.038
T_7	-0.214	0.107	0.069	GCP_7	-0.024	-0.034	-0.021
T_8	-0.167	0.206	0.064	GCP_8	-0.031	-0.027	-0.045
T_9	-0.068	0.135	0.119	GCP_9	0.032	0.046	-0.051
T_10	-0.118	0.098	0.088	GCP_10	0.022	0.037	0.029
T_11	-0.127	0.115	0.066	**RMSE**	**0.034**	**0.037**	**0.043**
T_12	-0.162	-0.139	0.136				
T_13	-0.114	-0.198	0.132				
RMSE	0.154	0.163	0.106				

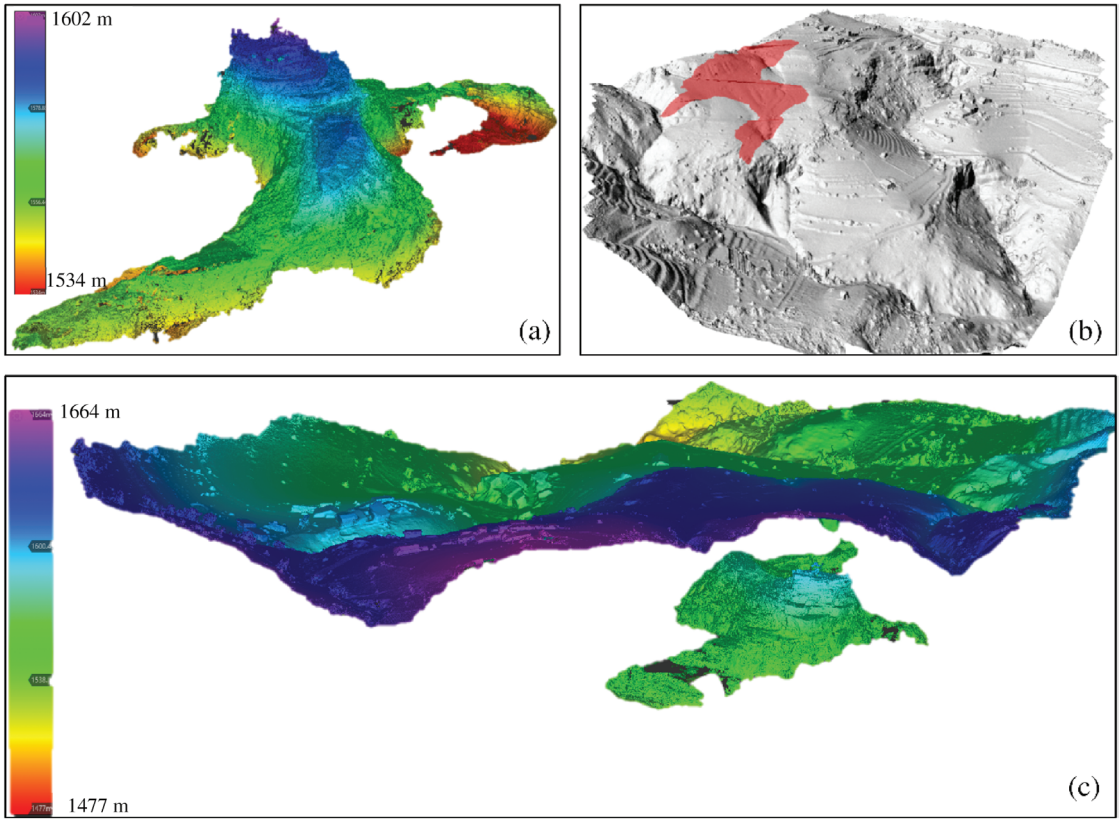

Fig. 6 Examples of the data obtained using TLS and UAV systems: (a) the Akcakale Cave TLS point cloud; (b) 3D representation of the cave projection on the hillshade generated from DSM; (c) integration of the UAV and TLS point clouds

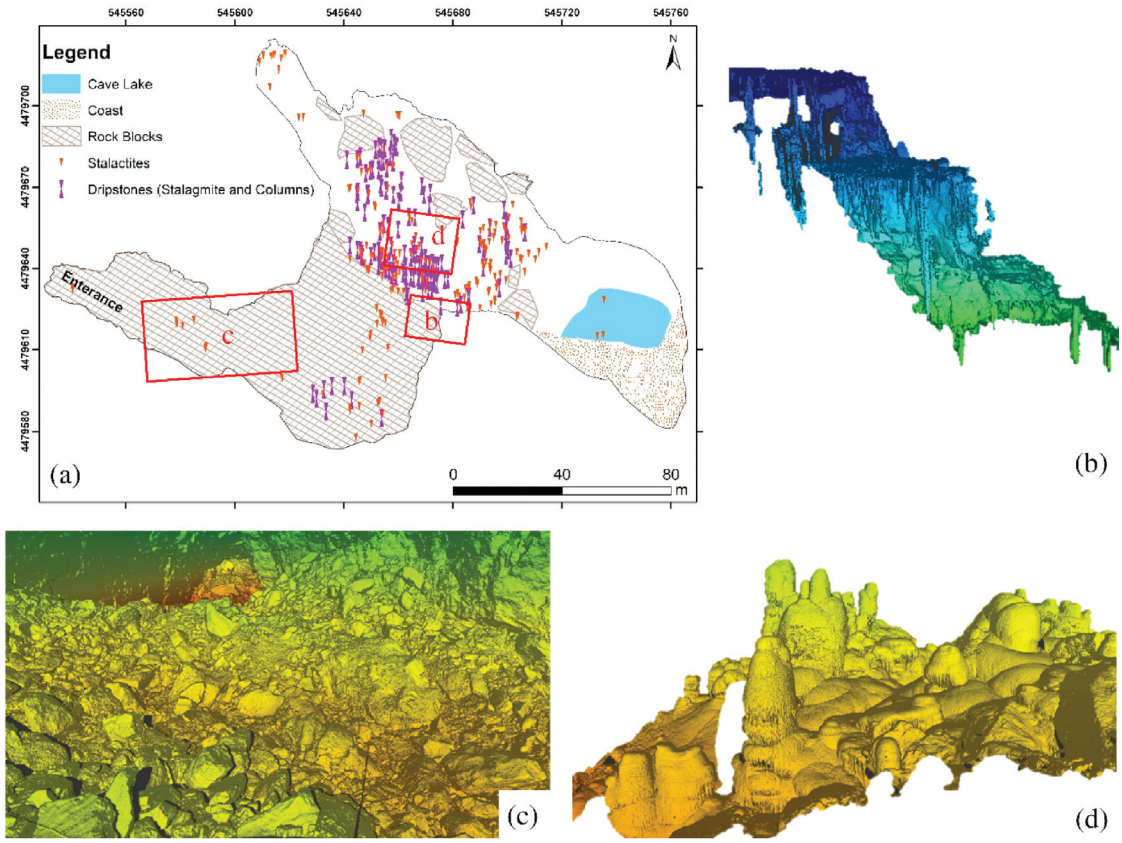

Fig. 7 Details of the Akcakale Cave created using the TLS point cloud: (a) 2D cave map, (b) 3D stalactite samples, (c) 3D rock blocks, (d) 3D dripstone formations on the cave floor

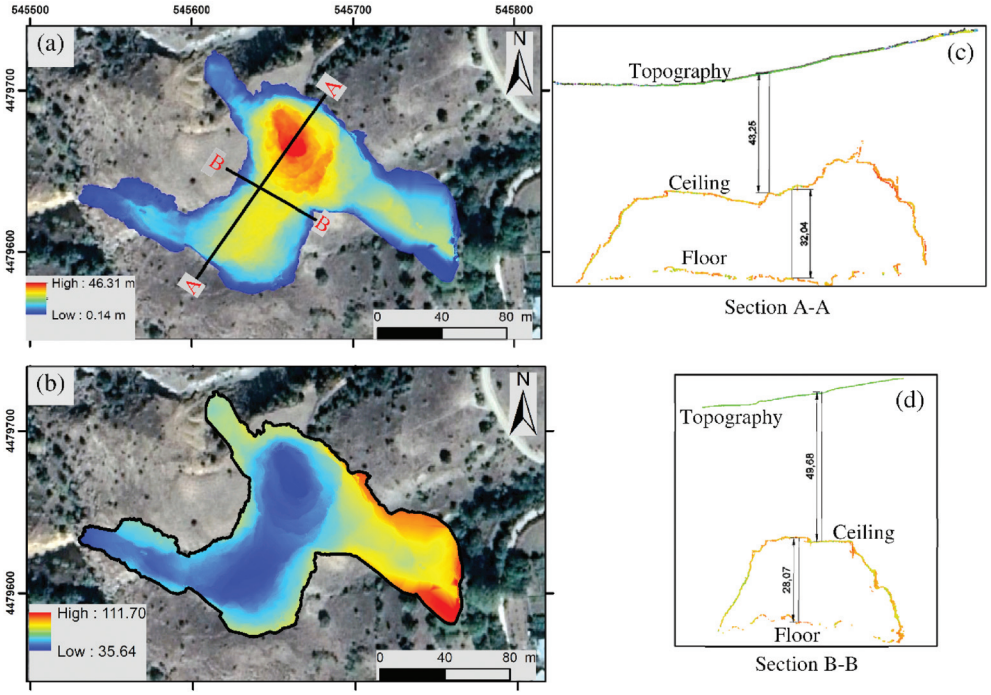

Fig. 8 UAV and TLS elevation models of the Akcakale cave and data generated from the integrated point clouds: (a) ceiling height, (b) depth from surface, (c, d) sample sections including cave and surface topography

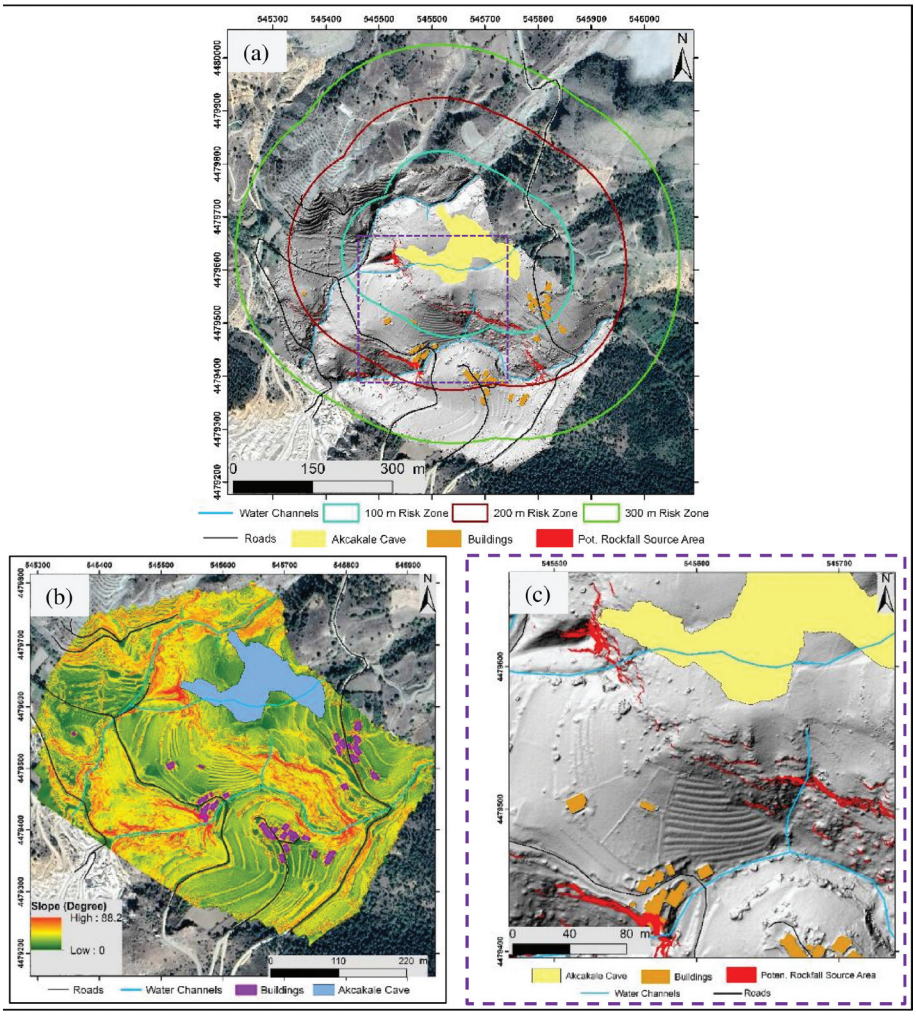

Fig. 9 Relationship of the Akçakale cave with its surface topography, (a) topography details and risk zones, (b) topography slope, and (c) source rock areas that may cause rockfalls in the vicinity of the cave

and the surface topography from the cave entrance to the area opening to the galleries was found to vary between 35 m and 50 m. The depth of the cave from the surface in the galleries increases in the northwestern and southeastern directions. The deepest (111.70 m) area between the cave and the surface was found at the end of the southeastern gallery. The volume of the limestone mass above the cave calculated from the elevation models of the cave ceiling and surface topography was found to be equal to 882 961.63 m^3. The longitudinal and cross-section examples showing the elevation change between the cave and the surface topography are presented in Figure 8c and Figure 8d, respectively. These sections are generated from the integrated TLS and UAV point clouds. The sections can be used for stability analysis, especially considering the actual cave size and load on the cave.

The buildings, roads, and water channels in the study area were digitized from the orthomosaic data derived from UAV images to determine the relationship between the cave and the surface topography. The source rock areas that may cause rockfalls in the study area were determined using UAV-DTM according to equation 1. The regions with an angle of more than 65° in the field were determined to be source rock areas. According to the cave plan, three risk zones were distinguished at 100 m intervals.The evaluation of the risk zones revealed that the southeastern gallery of the cave and the buildings north of the study area fall within the 100-meter risk zone. In this area, the closest building to the cave is approximately 35 m away (Fig. 9a). In this region, the cave is 110 m below the ground surface and the surface topography of the cave has almost the same elevation level as the nearest building (Fig. 9b). The buildings south and southeast of the cave are located within the 200 m and 300 m risk zones (Fig. 9a). There is a potential rock source area that causes potential rockfalls just above the remaining buildings south of the cave (Fig. 9c). In this area, the height of the cave ceiling is 20–30 m (Fig. 8a). The depth of the cave below the surface is about 35–50 m (Fig. 8b). The examination of the 2D map of the cave showed that the relevant part of the cave interior consists of rock blocks (Figs 7a and 7c), and its stability is weak. A collapse in this section may trigger the movement of the rock blocks in the southern part of the cave, causing damage to the buildings in these areas. The examination of the source rock areas that may cause potential rockfalls showed that intense source rock areas are at the entrance of the cave, which is because of the high slope (Figs 9b and 9c). In order to turn the cave into a tourist attraction and make it suitable for tourist activities in the future, it is of vital importance to develop protective measures against potential rockfalls in this region.

DISCUSSION

The use of TLS and UAV technology has made the measurement process of caves with complex geometry and difficult-to-access areas easier. The TLS with its light-free measurement capability and dense point cloud generation capacity is a useful system for producing detailed data for the cave interior, while UAVs are useful for mapping the surrounding topography outside the cave in terms of reducing the land surveying time and generating data from places inaccessible to humans. Combining the data of these two systems in a geo-located manner and presenting them in the GIS environment is important for documenting caves as well as for cave management and risk assessment purposes. The collected data are accurate within a small margin of error, making it suitable for 2D and 3D cave investigations. The relationship between the cave and the surface topography was established, and locations of the source rock and potential rockfalls were identified. These data can be used in the future to analyze cave stability, determine the protection boundary around the cave in case of possible risk, and to take the necessary measures to promote cave tourism in the area. When applied to such complicated geological structures as caves, the combined use of TLS and UAV technology has allowed collecting precise and important data that can improve our understanding of these features and the way they should be managed for the benefit of future generations. Prior to data collection using the TLS and UAV systems, a geodetic network was established in the study area so as to establish a common geodetic reference system for both TLS and UAV data. This allowed combining the TLS and UAV data and analyzing them together in a georeferenced and accurate manner. The ground-based geodetic network was established by installing reference points using the GNSS-RTK method and a laser total station, which extended from the entrance to the end of the cave. The total station measurements at each position were utilized to align the TLS point clouds to the geodetic reference system established by the TLS targets attached to the cave walls. To do the same with the data collected by the UAV, GCPs were set up outside the cave and measured using the GNSS-RTK method. By implementing this methodology, the TLS and UAV data were integrated and analyzed together, producing a complete and accurate map of the cave and its surroundings. The data produced by the UAV system had an expected level of error margin. However, the conversion of the point cloud of the TLS system to the geodetic coordinate system yielded a larger margin of error than expected. The margin of the error obtained from both systems is minimal enough not to affect the accuracy of the study. The georeferencing error of the

TLS survey inside the cave was higher than expected due to several factors, i.e., lightless environment, complex geometry, and difficult ground conditions inside the cave which made the terrestrial geodetic measurements challenging. The lightless environment made it difficult to capture accurate measurements, and the complex geometry and difficult ground conditions made it challenging to establish reference points for the system. Despite these challenges, the margins of error obtained from both the TLS and UAV systems were lower than 0.25 meter which is acceptable for most applications (Šašak *et al*. 2019; Domej *et al*. 2022). Overall, the combination of TLS and UAV systems in producing sensitive and accurate data for the cave interior and its surface topography was successful. Also, it should be noted that the TLS measurements are highly precise, as the TLS system measures the relative distances between each point with a millimeter accuracy at each station, however, the errors occur when rotating and translating the generated point cloud to align with the geodetic reference system. The data obtained can be useful for a variety of applications, including the cave stability analysis, determination of protection boundaries around the cave in case of risk, and the promotion of tourism in the cave. The 2D ground plan of the Akçakale cave was produced using the 3D point cloud data obtained with a TLS. The cave was found to cover an area of 13,750 m^2, which is smaller than the area of 18,000 m^2 previously calculated using classical measurement methods (Uzun, Zeybek 1996). The precision measurement systems used in this study provided a more accurate estimation of the cave area. The volume and ceiling heights of the cave were calculated using elevation models generated from the TLS point cloud data to understand the cave geometry. This information is valuable for understanding the size and shape of the cave and for identifying potential areas of instability. Locations of dripstones on the cave floor and ceiling as well as the boundaries of the rock blocks on the ground were precisely determined using the 3D point cloud data and mapped in the GIS environment. These data are sensitive and accurate enough to be used in determining safe walking routes if the cave is suitable for tourism in the future. Overall, the data obtained from the TLS measurements allowed for a more comprehensive understanding of the cave geometry and features, which can be useful for future management decisions and risk assessments. The precise measurements obtained in this study demonstrate the effectiveness of using modern surveying techniques to accurately document and analyze caves. In this study, the 3D data for both the cave interior and exterior, obtained using the TLS and UAV systems were integrated, and imported into the GIS environment. The data were then combined with various features such as buildings, roads, and water channels for the rockfall risk assessment and further investigations. The depth of the cave was determined using the TLS data, and the total load mass on the cave was calculated by integrating the TLS and UAV point clouds. Additionally, the source rock areas that may cause potential rockfall risk were identified around the cave. It was perceived that the source rock areas around the entrance of the cave and south of the cave are the most critical in terms of risk to visitors and nearby buildings when the cave is opened for tourism. The source rock areas around the entrance of the cave are dense enough to cause rockfalls, while the source rock areas in the southern part of the cave may pose a threat to the buildings in this area. To determine the potential rockfall risk more precisely, oblique images of the source rock areas will be taken with the UAV system in future studies. By using the data obtained from the oblique images, suspended blocks will be detected, and their rockfall risks will be determined more accurately (Zhan et al. 2022). Moreover, stability analysis will be made for each gallery of the cave with the sections to be produced from the integrated TLS and UAV point clouds. In this way, stability of the cave will be updated, which was previously analyzed based on the data obtained from conventional measurements. The updated stability analysis is critical for ensuring the safety of visitors and nearby buildings if the cave is opened for tourism. The data obtained from the integration of TLS and UAV point clouds can be used to determine the walking routes and the protection boundaries around the cave to reduce potential risks. These data can also be used to update the cave management plan, which is essential for preserving the natural and cultural heritage of the cave while promoting its tourism potential. In addition, stability analysis will be made for each gallery of the cave with the sections to be produced from the integrated TLS and UAV point clouds, and the stability of the cave, which was previously analyzed based on the data produced by conventional measurements (Alemdag *et al*. 2019), will be updated. Overall, the integrated 3D data of the cave and its surroundings in the GIS environment, in combination with the mapping of various features in the field, have provided valuable information for assessing the rockfall risk and for further investigations.

CONCLUSION

The objective of this study was to map the Akçakale cave in detail and to integrate both inside and outside topography data in the GIS environment, using the TLS and UAV systems, in order to produce high-accuracy data for cave management and risk

assessment. The mapping process involved producing 2D data such as cave plans and surface topography details, and 3D data such as the volume, height, depth, and rock areas that may cause rockfall. The TLS system was used to create a detailed 3D point cloud of the cave interior, and the UAV system was utilized to generate a 3D model of the surface topography. These two systems were combined using a geodetic network established in the study area, providing a common geodetic reference system for both TLS and UAV data. The obtained data can be used for cave stability analysis, rockfall risk assessment, cave interior, and surface topography management, and the production of cave management plans in the GIS environment.

The study revealed that the cave has an area of 13,750 m^2, which is smaller than the previous estimate of 18,000 m^2 obtained using conventional measurement methods. The volume and ceiling heights of the cave were calculated using elevation models produced from the TLS point cloud. The 3D point cloud data were also used to map locations of dripstones on the floor and ceiling of the cave, and the boundaries of the rock blocks on the ground were precisely determined. These data can be used in the future to determine walking routes if the cave is deemed suitable for tourism. The study also identified potential risks associated with the cave, particularly the risk of rockfall in the source rock areas around the cave entrance and the southern part of the cave. The nearest building to the cave is approximately 35 meters away, and all the buildings in the area are less than 300 meters from the cave. In the event of a cave collapse, the buildings in the southern part of the cave are at risk of rockfall. It is recommended that the cave entrance be improved with rockfall prevention structures before it is opened to tourism.

In conclusion, the combination of TLS and UAV technologies has enabled a comprehensive mapping of the Akcakale cave and its surrounding topography, yielding accurate and highly detailed data for cave management and risk assessment. The data from this study can be used for GIS-based cave stability analysis, rockfall risk assessment, and the design of cave management strategies. The study also identified potential risks associated with the cave, namely the risk of rockfall in the source rock areas surrounding the cave entrance and in the southern portion of the cave, highlighting the necessity of implementing rockfall prevention structures prior to opening the cave to tourists. The contribution of this work is the demonstration of the effectiveness of combining current surveying techniques to provide detailed and precise data for cave mapping and management, which can inspire future studies and management decisions to preserve and promote the natural and cultural heritage of caves.

ACKNOWLEDGMENTS

The authors would like to express their sincere gratitude to the anonymous reviewers for their valuable comments, suggestions, and critiques, which significantly contributed to improving the quality of this manuscript. The feedback and constructive criticism provided by the reviewers were instrumental in shaping the final version of this paper. The authors also wish to acknowledge the support of their respective institutions and colleagues who assisted in the completion of this research.

REFERENCES

Albert, G. 2017. Aspects of cave data use in a GIS. *Cave Investigations (Intech, Rijeka),* https://doi.org/10./intechopen

Alemdag, S., Zeybek, H.İ., Kulekci, G. 2019. Stability evaluation of the Gümüşhane-Akçakale cave by numerical analysis method. *Journal of Mountain Science 16 (9),* 2150–2158, https://doi.org/10.1007/s11629-019-5529-1

Alessandri, L., Baiocchi, V., Del Pizzo, S., Di Ciaccio, F., Onori, M., Rolfo, M.F., Troisi, S. 2020. The fusion of external and internal 3D photogrammetric models as a tool to investigate the ancient human/cave interaction: The La Sassa case study. *International Archives of the Photogrammetry, Remote Sensing and Spatial Information Sciences 43, B2–2020,* https://doi.org/10.5194/isprs-archives-XLIII-B2-2020-1443-2020

Armstrong, B.J., Blackwood, A.F., Penzo-Kajewski, P., Menter, C.G., Herries, A.I. 2018. Terrestrial laser scanning and photogrammetry techniques for documenting fossil-bearing palaeokarst with an example from the Drimolen Palaeocave System, South Africa. *Archaeological Prospection 25,* 45–58, https://doi.org/10.1002/arp.1580

Bauerhansl, C., Frederic, B., Luuk, D., Philippe, D., Christian, G., Karl, K., Valerie, K., Tatjana, K., Matteo, M., Frank, P. 2010. Development of harmonized indicators and estimation procedures for forests with protective functions against natural hazards in the alpine space (PROALP). *Institute for Environment and Sustainability. Office for Official Publications of the European Communities.© European Communities,* https://doi.org/10.2788/51473

Chaudhry, M.H., Ahmad, A., Gulzar, Q. 2020. Impact of UAV surveying parameters on mixed urban landuse surface modelling. *ISPRS International Journal of Geo-Information 9 (11),* 656, https://doi.org/10.3390/ijgi9110656

De Waele, J., Fabbri, S., Santagata, T., Chiarini, V., Columbu, A., Pisani, L. 2018. Geomorphological and speleogenetical observations using terrestrial laser scanning and 3D photogrammetry in a gypsum cave (Emilia Romagna, N. Italy), *Geomorphology 319,* 47–61, https://doi.org/10.1016/j.geomorph.2018.07.012

Domej, G., Previtali, M., Castellanza, R., Spizzichino, D., Crosta, G.B., Villa, A., Fusi, N., Elashvili, M., and Margottini, C. 2022. High-Resolution 3D FEM Stability Analysis of the Sabereebi Cave Monastery, Georgia. *Rock Mechanics and Rock Engineering 1–24,* https://doi.org/10.1007/s00603-022-02858-z

Fabbri, S., Sauro, F., Santagata, T., Rossi, G., De Waele, J. 2017. High-resolution 3-D mapping using terrestrial laser scanning as a tool for geomorphological and speleogenetical studies in caves: An example from the Lessini mountains (North Italy), *Geomorphology 280,* 16–29, http://dx.doi.org/10.1016/j.geomorph.2016.12.001

Gallay, M., Kaňuk, J., Hochmuth, Z., Meneely, J.D., Hofierka, J., Sedlák, V. 2015. Large-scale and high-resolution 3-D cave mapping by terrestrial laser scanning: a case study of the Domica Cave, Slovakia. *International Journal of Speleology 44,* 6, http://dx.doi.org/10.5038/1827-806X.44.3.6

Hoffmeister, D., Zellmann, S., Pastoors, A., Kehl, M., Cantalejo, P., Ramos, J., Weniger, G., Bareth, G. 2016. The investigation of the Ardales Cave, Spain-3D documentation, topographic analyses, and lighting simulations based on terrestrial laser scanning. *Archaeological Prospection 23,* 75–86, https://doi.org/10.1002/arp.1519

Hu, S., Qiu, H., Wang, N., Cui, Y., Wang, J., Wang, X., Ma, S., Yang, D., Cao, M. 2020. The influence of loess cave development upon landslides and geomorphologic evolution: A case study from the northwest Loess Plateau, China. *Geomorphology 359,* 107167, https://doi.org/10.1016/j.geomorph.2020.107167

Idrees, M.O., Pradhan, B. 2016. A decade of modern cave surveying with terrestrial laser scanning: A review of sensors, method and application development. *International Journal of Speleology 45,* 8, http://dx.doi.org/10.5038/1827-806X.45.1.1923

Idrees, M.O., Pradhan, B. 2018. Geostructural stability assessment of cave using rock surface discontinuity extracted from terrestrial laser scanning point cloud. *Journal of Rock Mechanics and Geotechnical Engineering 10,* 534–44, https://doi.org/10.1016/j.jrmge.2017.11.011

Le, V.C., Cao, X.C., Nguyen, Q.L., Le, T.T.H., Tran, T.A., Bui, X.N. 2020. Experimental investigation on the performance of DJI phantom 4 RTK in the PPK mode for 3D mapping open-pit mines. *Inżynieria Mineralna,* http://dx.doi.org/10.29227/IM-2020-02-10

Leica Geosystems AG. 2011. Leica ScanStation C10. The All-in-One Laser Scanner for Any Application datasheet., Leica Geosystems AG, Heerbrugg, Switzerland. Available online: https://leica-geosystems.com/SFTP/files/archived-files/Leica_ScanStation_C10_DS_sv.pdf

Lindgren, S., Galeazzi, F. 2013. 3D laser scanning in cave environment: The case of las cuevas, Belize acquisition of the cave system and excavation area, Digital Heritage. *International Congress (Digital Heritage) 1,* 219–222. *IEEE*, https://doi.org/10.1109/DigitalHeritage.2013.6743737

Öztürk, O., Bilgilioğlu, B.B., Çelik, M.F., Bilgilioğlu, S.S., Uluğ, R. 2017. The Investigation of The Height and The Camera Angle in The Production of Orthoimage with Images of Unmanned Aerial Vehicle (UAV). *Geomatik 2 (3),* 135–142, https://dergipark.org.tr/tr/download/article-file/342914

Pukanská, K., Barto , K., Bella, P., Ga inec, J., Blistan, P., Kovanič, Ľ. 2020. Surveying and high-resolution topography of the ochtiná aragonite cave based on tls and digital photogrammetry. *Applied Sciences 10,* 4633, https://doi.org/10.3390/app10134633

Sam, L., Bhardwaj, A., Singh, S., Martin-Torres, F.J., Zorzano, M.P., Ramírez Luque, J.A. 2020. Small lava caves as possible exploratory targets on Mars: Analogies drawn from UAV imaging of an Icelandic lava field. *Remote Sensing 12,* 1970, https://doi.org/10.3390/rs12121970

Šašak, J., Gallay, M., Kaňuk, J., Hofierka, J., Minár, J. 2019. Combined Use of Terrestrial Laser Scanning and UAV Photogrammetry in Mapping Alpine Terrain. *Remote Sensing 11*, 2154, https://doi.org/10.3390/rs11182154

Šupinský, J., Kaňuk, J., Nováková, M., Hochmuth, Z. 2022. LiDAR point clouds processing for large-scale cave mapping: a case study of the Majko dome in the Domica cave. *Journal of Maps,* 1–8, https://doi.org/10.1080/17445647.2022.2035270

Uzun, A., Zeybek, H.İ. 1996. Akçakale Mağarası (Gümüşhane). *Türk Coğrafya Dergisi,* 39–53, https://dergipark.org.tr/tr/pub/tcd/issue/21256/228113

Zhan, J., Yu, Z., Lv, Y., Peng, J., Song, S., Yao, Z. 2022. Rockfall Hazard Assessment in the Taihang Grand Canyon Scenic Area Integrating Regional-Scale Identification of Potential Rockfall Sources. *Remote Sensing 14 (13),* 3021, https://doi.org/10.3390/rs14133021

Žabota, B., Repe, B., Kobal, M. 2019. Influence of digital elevation model resolution on rockfall modelling. *Geomorphology 328,* 183–195, https://doi.org/10.1016/j.geomorph.2018.12.029